recycling

MDPI

*Article*

# Silver Leaching from Waste Mobile-Phone Printed Circuit Boards Using Choline Chloride-Based Deep Eutectic Solvents and Subsequent Dissolved-Silver Removal

**Esteban Morales [1], Katherine Moreno [1,*], Fernando Sánchez [1], Ernesto de la Torre [1], Pía Hernández [2] and Carlos F. Aragón-Tobar [1]**

[1] Department of Extractive Metallurgy, Escuela Politécnica Nacional, Ladrón de Guevara E11-253, P.O. Box 17-01-2759, Quito 170525, Ecuador; esteban.morales01@epn.edu.ec (E.M.); fernando.sanchez01@epn.edu.ec (F.S.); ernesto.delatorre@epn.edu.ec (E.d.l.T.); carlos.aragont@epn.edu.ec (C.F.A.-T.)

[2] Department of Chemical and Mineral Processes, Universidad de Antofagasta, Av. Universidad de Antofagasta 02800, Antofagasta 1271155, Chile; pia.hernandez@uantof.cl

* Correspondence: katherine.moreno@epn.edu.ec; Tel.: +593-983-467-654

**Abstract**

The increasing generation of waste electrical and electronic equipment (WEEE) has intensified the need for environmentally safer processes to recover valuable metals from secondary resources. Post-consumer mobile-phone printed circuit boards (PCBs) are particularly relevant due to their elevated silver content. This study evaluated silver extraction from two categories of mobile-phone PCBs, traditional-architecture devices with physical keyboards and new-generation touchscreen devices, using choline chloride-based deep eutectic solvents (DESs). After dismantling, comminution, and particle-size classification, the PCB fractions were characterized by fire assay and atomic absorption spectrometry. The recalculated silver grades were 142.5 g $t^{-1}$ for traditional-architecture PCBs and 569.3 g $t^{-1}$ for new-generation PCBs, demonstrating a strong dependence on device architecture. Three DESs were evaluated: acetine (choline chloride–acetic acid), ethaline (choline chloride–ethylene glycol), and oxaline (choline chloride–oxalic acid). Leaching experiments were conducted at 40 °C for 24 h. Acetine exhibited the highest silver-leaching efficiencies, reaching 71.5% for traditional-architecture PCBs and 60.8% for new-generation PCBs. Silver was subsequently recovered from the loaded acetine by cementation with metallic iron. This method achieved 98.8% silver recovery in the reference system and 84.8% in the real PCB leachate. These results demonstrate the workability of acetine-mediated silver recovery from post-consumer mobile-phone PCBs.

**Keywords:** silver; deep eutectic solvents; printed circuit boards; e-waste; recovery

Check for updates

Academic Editor: Ana Paula Paiva

Received: 30 September 2026
Revised: 10 November 2026
Accepted: 18 November 2026
Published: 26 November 2026

**Copyright:** © 2026 by the authors. Licensee MDPI, Basel, Switzerland. This article is an open access article distributed under the terms and conditions of the Creative Commons Attribution (CC BY) license.

## 1. Introduction

Global industrial demand for silver exceeded 650 million troy ounces in 2023, driven largely by the expansion of emerging technologies and applications in the electronics and energy sectors [1]. Silver is widely used in electrical contacts, solders, multilayer ceramic capacitors (MLCCs), and photovoltaic cells because of its high electrical and thermal conductivity, corrosion resistance, and reliable performance in conductive components [2,3]. The sustained growth of these applications has increased pressure on the silver supply chain and reinforced the need to recover this metal from secondary resources.

Silver recovery from waste electrical and electronic equipment (WEEE) must be considered in the context of the broader challenge of rapidly increasing global electronic-waste generation. Worldwide e-waste generation reached 62 million tonnes in 2022, representing an increase of approximately 82% compared with 2010, and is projected to reach 82 million tonnes by 2030 [4]. This growth has substantially outpaced formal recycling capacity. Only 22.3% of the e-waste generated in 2022 was documented as formally collected and recycled in an environmentally sound manner, and this proportion is projected to decrease to 20% by 2030 [4]. In addition to the associated environmental burden, the current recycling gap represents approximately USD 62 billion in potentially recoverable metals and materials that remain unexploited each year [4,5]. These data highlight the need to develop efficient and accessible processes to recover valuable metals from secondary resources, such as post-consumer mobile-phone printed circuit boards (PCBs).

Among the different WEEE streams, post-consumer mobile phones constitute a secondary resource of considerable metallurgical interest. A mobile phone can contain up to 40 elements, including precious metals such as gold, silver, and palladium [6]. Silver is mainly concentrated in PCBs, where its content can reach approximately 0.12 wt.% [7], with reported grades ranging from 520 to 2901 g $t^{-1}$ [8]. These values can be considerably higher than those of primary silver ores. For example, a major silver mining project in Mexico has a reported average silver grade of 102 g $t^{-1}$ Ag [9]. However, the concentration and distribution of silver in mobile-phone PCBs vary by manufacturer, model, components, and the device's technological architecture. In particular, differences have been reported between feature phones equipped with physical keyboards and newer touchscreen smartphones [6].

The economic attractiveness of recycling mobile-phone PCBs is also influenced by the technological evolution of these devices. An economic assessment of 14 WEEE categories showed that smartphones contain a higher concentration of valuable materials per unit mass than earlier feature-phone designs, positioning them among the potentially most profitable electronic-waste streams under projected generation scenarios [10]. Nevertheless, the transition toward increasingly compact and integrated devices can complicate dismantling and the physical liberation of metal-bearing components. A similar effect has been observed when comparing tablets with notebook computers [10]. Consequently, the increasing value concentration in newer devices may be accompanied by greater processing complexity. This trade-off supports classifying post-consumer mobile phones by their technological architecture prior to metallurgical treatment.

Silver can be recovered from PCBs through pyrometallurgical, hydrometallurgical, or combined processing routes [11]. Pyrometallurgical processes can treat large quantities of heterogeneous material and achieve high metal recoveries. However, exposing the polymeric fraction of PCBs to high temperatures can generate hazardous emissions, including dioxins and other organochlorine compounds, unless advanced gas-treatment systems are employed [12]. Hydrometallurgical processing, in contrast, generally operates at lower temperatures and can provide greater selectivity through controlled leaching and solution-purification stages. Nevertheless, conventional lixiviants used for silver recovery, including nitric acid, aqua regia, and cyanide-containing solutions, present substantial environmental, occupational, and operational risks [13,14]. Therefore, research has increasingly focused on alternative leaching systems that combine metal extraction efficiency with improved environmental performance.

Biodegradable organic acids, including oxalic, citric, and malic acids, have been shown to leach metals such as cobalt, lithium, nickel, and silver from secondary resources [15,16]. Deep eutectic solvents (DESs) represent another emerging class of alternative leaching media. These solvents are generally formed by combining a hydrogen-bond acceptor (HBA) with a hydrogen-bond donor (HBD), producing a mixture with a melting point substantially

lower than that of its individual components [17]. DESs typically exhibit low volatility and highly tunable physicochemical properties. However, their cost, toxicity, biodegradability, viscosity, and recyclability depend on the chemical identity and proportions of their constituent compounds; therefore, their environmental suitability must be evaluated for each specific formulation and application [18].

Since the first reported choline chloride-based DES [19], choline chloride (ChCl) has become one of the most widely investigated HBAs in solvometallurgical applications due to its availability, relatively low cost, and favorable toxicological profile compared with many conventional ionic liquid components [20]. ChCl-based systems such as ethaline (ChCl–ethylene glycol), reline (ChCl–urea), and oxaline (ChCl–oxalic acid) have been investigated for extracting metals from primary and secondary resources, with silver-leaching efficiencies of up to 100% reported under temperatures ranging from 40 to 100 °C [21]. Ethaline has achieved silver-leaching efficiencies of up to 99.9% from photovoltaic cells [22] and gold extraction efficiencies of 71.9% from mine tailings [23]. Oxaline has also been applied to spent lithium-ion batteries, achieving lithium extraction efficiencies above 80%, although cobalt extraction remained below 50% under the evaluated conditions [24].

Despite these advances, the use of ChCl-based DESs for the direct extraction of silver from post-consumer mobile-phone PCBs remains underexplored. In particular, the DES formed by ChCl and acetic acid, referred to as acetine in the present study, is less documented than ethaline and oxaline. Previous research demonstrated its ability to extract Cu, Ni, and Au from PCBs when iodine was incorporated as an oxidizing agent [25].

Conventional hydrometallurgical processing has demonstrated that silver can be effectively recovered from waste PCBs. For example, approximately 98 wt.% of the input silver was recovered during aqua regia treatment of waste PCBs, while gold and palladium were separated through additional recovery stages [26]. However, the recovery behavior of dissolved silver from DES-based leachates remains underexplored.

The recovery of silver from the loaded DES is a critical downstream operation because it determines the form of the recovered product and the overall efficiency and selectivity of the process. Chemical precipitation has also been investigated as an alternative method for silver recovery from leaching solutions, with reported efficiencies of up to 99.9% [27]. However, its effectiveness in complex leachates may be influenced by the presence of other dissolved metals, which can affect recovery selectivity and product purity.

Alternatively, silver can be recovered by cementation with metallic iron, a process that relies on the spontaneous oxidation of iron and the simultaneous reduction of dissolved-silver species. Although cementation is a relatively simple and well-established metal-recovery technique in hydrometallurgy, its application in deep eutectic solvent (DES) media remains underexplored. In particular, the relatively high viscosity of many DES formulations may limit mass transfer between dissolved metal species and the cementing agent, potentially affecting recovery efficiency [28,29]. Furthermore, the presence of other dissolved metals in complex PCB leachates may influence the selectivity of the cementation process.

Accordingly, this study evaluated an integrated hydrometallurgical route for recovering silver from post-consumer mobile-phone PCBs, which were classified into two technological categories: feature phones with physical keyboards and newer-generation touchscreen smartphones. First, granulochemical characterization was performed to determine the distribution of silver among the particle-size fractions of each PCB category. The silver-rich fractions were subsequently treated with three ChCl-based DESs containing acetic acid, ethylene glycol, or oxalic acid as hydrogen-bond donors. Finally, silver recovery from the best-performing DES was evaluated by iron cementation, using both a silver reference system and a real PCB leachate. This approach enabled comparison of silver-leaching performance among the three DES formulations and evaluation of silver recovery

efficiency via cementation with metallic iron in a complex leachate derived from waste printed circuit boards.

The scope of this study is limited to the granulochemical distribution, DES leaching, and subsequent recovery of silver from post-consumer mobile-phone PCBs. The behavior and recovery of other metals present in the PCB matrix were not systematically investigated. Accordingly, this study evaluated the granulochemical distribution and DES leaching of silver from two categories of post-consumer mobile-phone PCBs. Three ChCl-based DESs containing acetic acid, ethylene glycol, or oxalic acid as hydrogen-bond donors were compared. Acetine, the best-performing DES, was subsequently evaluated in an exploratory iron-treatment experiment to determine the decrease in dissolved-silver concentration.

## 2. Results

### *2.1. Granulochemical Characterization of Silver in Mobile-Phone PCBs*

The granulochemical characterization showed marked differences in both silver grade and particle-size distribution between traditional-architecture and new-generation mobile-phone PCBs. The results for each category are presented in Figure 1 below.

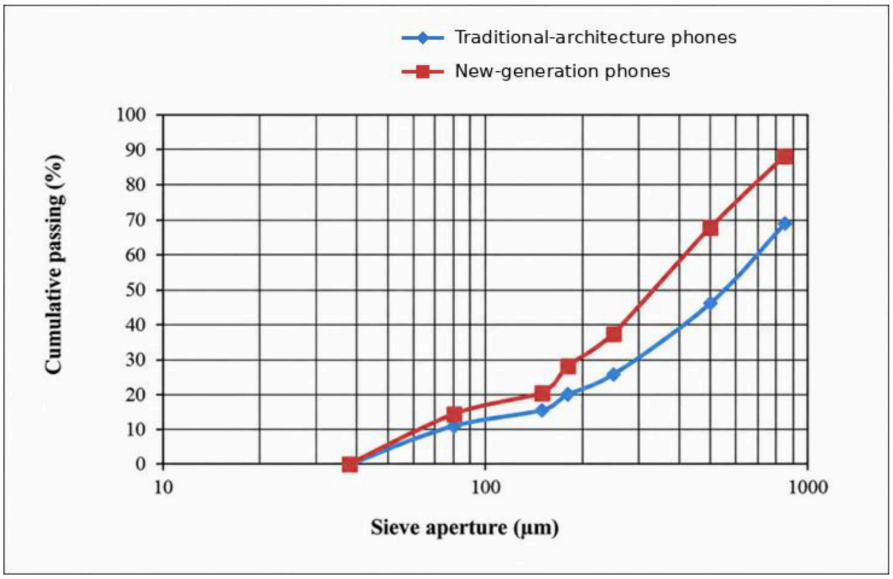


**Figure 1.** Silver-leaching efficiency as a function of time for traditional-architecture mobile-phone PCB fines using acetine, ethaline, and oxaline. Experimental conditions: 2 wt.% solids, 40 °C, 400 rpm, and 24 h.

#### 2.1.1. Traditional-Architecture Phones

Table 1 presents the silver grades determined for the different particle-size fractions of traditional-architecture mobile-phone PCBs. Silver was detected in all the fractions analyzed, although its concentration varied considerably with particle size.

The highest silver grade was measured in the #100-mesh fraction at 656.2 g $t^{-1}$, followed by the #180-mesh fraction at 560.6 g $t^{-1}$. The fines (<85 µm) also presented a relatively high silver grade of 358.1 g $t^{-1}$. By contrast, the lowest grades were observed in the #35- and #80-mesh fractions, at 3.2 and 3.3 g $t^{-1}$, respectively. The recalculated silver grade of the complete sample was 142.5 g $t^{-1}$.

**Table 1.** Silver grades by particle-size fraction in traditional-architecture mobile-phone PCBs.

| Mesh | Opening (μm) | Ag (g ton$^{-1}$) |
|---|---|---|
| #20 | 850 | 76.8 |
| #35 | 425 | 3.2 |
| #60 | 250 | 116.7 |
| #80 | 180 | 3.3 |
| #100 | 150 | 656.2 |
| #180 | 85 | 560.6 |
| Fines | <85 | 358.1 |
| Recalculated feed | - | 142.5 |

The distribution of silver among the particle-size fractions was calculated from the mass retained in each fraction and its corresponding silver grade. The results are presented in Table 2.

**Table 2.** Silver distribution by particle-size fraction in traditional-architecture mobile-phone PCBs.

| Mesh | Opening (μm) | Ag Composition (%) |
|---|---|---|
| #20 | 850 | 16.8 |
| #35 | 425 | 0.5 |
| #60 | 250 | 16.7 |
| #80 | 180 | 0.1 |
| #100 | 150 | 20.5 |
| #180 | 85 | 17.8 |
| Fines | <85 | 27.6 |
| Total | - | 100.0 |

The fines contained the largest share of silver, accounting for 27.6% of the sample's total silver. The #100 and #180 mesh fractions contained an additional 20.5% and 17.8%, respectively. Collectively, the fractions with particle sizes below 150 μm accounted for 65.9% of the total silver. In contrast, the #35- and #80-mesh fractions contributed only 0.5% and 0.1%, respectively.

#### 2.1.2. New-Generation Phones

The silver grades determined for new-generation mobile-phone PCBs are presented in Table 3. In contrast to traditional-architecture PCBs, silver was strongly concentrated in a single intermediate particle-size fraction.

**Table 3.** Silver grades by particle-size fraction in new-generation mobile-phone PCBs.

| Mesh | Opening (μm) | Ag (g ton$^{-1}$) |
|---|---|---|
| 20 | 850 | 0.0 * |
| 35 | 425 | 0.0 * |
| 60 | 250 | 1668.7 |
| 80 | 180 | 3.1 |
| 100 | 150 | 27.3 |
| 180 | 85 | 0.0 * |
| Fines | <85 | 428.1 |
| Recalculated feed | - | 569.3 |

* No quantifiable doré bead was obtained during fire assay. A value of 0.0 g t$^{-1}$ was assigned to complete the granulochemical balance.

The #60-mesh fraction had the highest silver grade, reaching 1668.7 g t$^{-1}$. The fines had the second-highest grade at 428.1 g t$^{-1}$, whereas the #80- and #100-mesh fractions contained

only 3.1 and 27.3 g $t^{-1}$, respectively. No quantifiable doré bead was obtained from the #20-, #35-, or #180-mesh fractions during the fire assay. Consequently, a value of 0.0 g $t^{-1}$ was assigned to these fractions for the calculation of the granulochemical balance.

The recalculated silver grade for the complete new-generation PCB sample was 569.3 g $t^{-1}$, approximately four times the value obtained for traditional-architecture PCBs.

Table 4 presents the distribution of silver across the particle-size fractions of the new-generation PCBs.

**Table 4.** Silver distribution by particle-size fraction in new-generation mobile-phone PCBs.

| Mesh | Opening (µm) | Ag Composition (%) |
|---|---|---|
| #20 | 850 | 0.0 |
| #35 | 425 | 0.0 |
| #60 | 250 | 88.8 |
| #80 | 180 | 0.1 |
| #100 | 150 | 0.4 |
| #180 | 85 | 0 |
| Fines | <85 | 10.8 |
| Total | - | 100.0 * |

* The sum of the individually rounded values may differ slightly from 100%.

The #60-mesh fraction accounted for 88.8% of the total silver in the new-generation PCB sample, indicating that silver was highly concentrated in this particle-size range. The fines accounted for a further 10.8%, whereas the contributions of the remaining fractions were each below 0.5%.

#### 2.1.3. Selection of the Fraction for DES Leaching

Although the #60-mesh fraction of the new-generation PCBs exhibited the highest silver grade and accounted for most of the silver in this category, the fine fraction (<85 µm) was selected for the DES leaching experiments in both PCB categories. This selection considered the smaller particle size, potential interference from other metallic species, and the need to ensure comparable experimental conditions across the two PCB categories. Smaller particles generally provide a larger specific surface area and shorter internal diffusion distances, potentially favoring solid–liquid contact and metal dissolution [30]. However, the influence of particle size on leaching kinetics was not experimentally evaluated in this study.

The fines presented appreciable silver grades of 206 g $t^{-1}$ in traditional-architecture PCBs and 428.1 g $t^{-1}$ in new-generation PCBs. During fire assay, these fractions produced doré beads directly, without forming the copper sponge observed in some coarser fractions, indicating comparatively lower copper interference. Furthermore, the smaller particle size provided a consistent feed for comparing the three DES systems under identical operating conditions. Therefore, the fines were selected as a technically suitable fraction for evaluating silver leaching from both PCB categories.

### *2.2. Silver Leaching with Deep Eutectic Solvents*

#### 2.2.1. Density of the Prepared DESs

The densities of acetine, ethaline, and oxaline were measured at 25 °C before the leaching experiments. The results are presented in Table 5.

**Table 5.** Density of the prepared deep eutectic solvents at 25 °C.

| DES | Components | Density (g mL$^{-1}$) |
|---|---|---|
| ACETINE | ChCl–acetic acid | 1.0940 |
| ETHALINE | ChCl–ethylene glycol | 1.1034 |
| OXALINE | ChCl–oxalic acid | 1.1828 |

Acetine exhibited the lowest density, followed by ethaline, whereas oxaline presented the highest density. The values ranged from 1.0940 to 1.1828 g mL$^{-1}$.

The measured densities of the prepared DESs ranged from 1.0940 to 1.1828 g mL$^{-1}$ at 25 °C. Acetine, ethaline, and oxaline exhibited densities of 1.0940, 1.1034, and 1.1828 g mL$^{-1}$, respectively. Acetine and ethaline showed similar density values, whereas oxaline exhibited the highest density among the investigated systems.

The density measured for acetine (ChCl:acetic acid, 1:2) was close to the value of 1.10944 g mL$^{-1}$ reported by Sheikh et al. for the same DES composition at 25 °C. Likewise, the density obtained for ethaline (ChCl:ethylene glycol, 1:2) was comparable to the value of 1.10202 g mL$^{-1}$ reported by Leron et al. at the same temperature. The density of oxaline (ChCl:oxalic acid, 1:1) was also consistent with the range of 1.04–1.24 g mL$^{-1}$ reported by Sibiya et al. for this type of DES. These comparisons suggest that the prepared solvents exhibited physicochemical properties consistent with those reported in the literature for similar systems.

Since replicate density measurements were not performed, the reported values should be considered descriptive and no inference regarding statistical significance is made.

### 2.2.2. Silver-Leaching Performance and Comparison Between PCB Categories

Figure 2 compares the silver-leaching efficiencies of traditional-architecture and new-generation PCB fines using acetine, ethaline, and oxaline over 24 h. All experiments were conducted using 2 wt.% solids at 40 °C and 400 rpm.

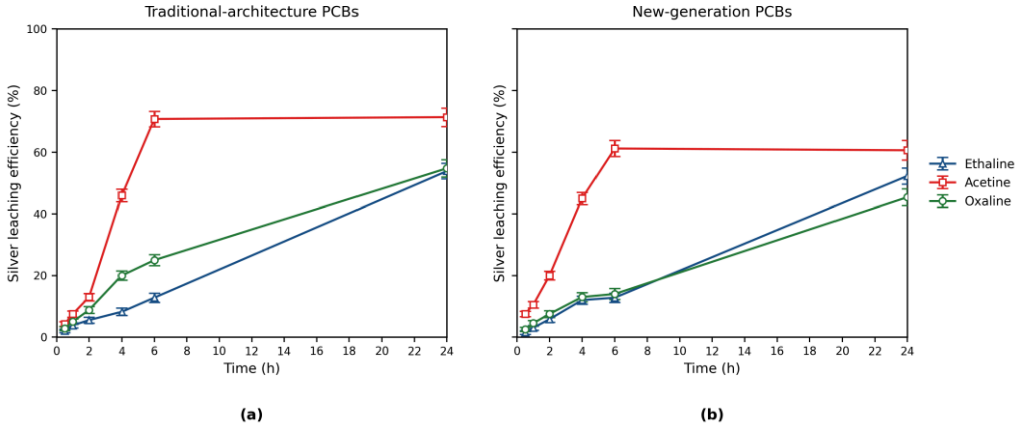


**Figure 2.** Silver-leaching efficiency as a function of time for fines from (**a**) traditional-architecture and (**b**) new-generation mobile-phone PCBs using acetine, ethaline, and oxaline. Experimental conditions: 2 wt.% solids, 40 °C, 400 rpm, and 24 h.

Acetine exhibited the fastest silver dissolution and highest final leaching efficiency in both PCB categories, reaching 71.5% for traditional-architecture PCBs and 60.8% for new-generation PCBs after 24 h. Most silver dissolution occurred within the first 6 h, reaching 70.8% and 61.4%, respectively, after which dissolution appeared to plateau.

In contrast, ethaline and oxaline exhibited slower dissolution, with silver-leaching efficiencies continuing to increase throughout the experimental period. After 24 h, ethaline

achieved efficiencies of 53.8% and 51.9% for traditional-architecture and new-generation PCBs, respectively, whereas oxaline achieved efficiencies of 54.9% and 45.4%.

As summarized in Table 6, all three DESs exhibited higher silver-leaching efficiencies for traditional-architecture PCBs than for new-generation PCBs. The differences between categories were 1.9, 10.7, and 9.5 percentage points for ethaline, acetine, and oxaline, respectively.

**Table 6.** Silver-leaching efficiencies after 24 h for the three DESs and both mobile-phone PCB categories.

| DES System | % Ag Recovery (Traditional Architecture) | % Ag Recovery (New Generation) |
|---|---|---|
| ETHALINE | 53.8 | 51.9 |
| ACETINE | 71.5 | 60.8 |
| OXALINE | 54.9 | 45.4 |

Based on its higher leaching efficiency and faster silver dissolution, acetine was selected for subsequent silver recovery experiments. Although traditional-architecture PCBs exhibited higher leaching efficiency, the acetine leachate from new-generation PCB fines was selected for cementation experiments because of its higher initial silver grade (428.1 g $t^{-1}$ compared with 206 g $t^{-1}$), which resulted in a slightly higher dissolved-silver concentration under the evaluated conditions.

#### 2.2.3. Comparison of Silver Leaching Between PCB Categories

Table 6 summarizes the silver-leaching efficiencies obtained after 24 h for the three DESs and the two PCB categories.

Acetine achieved the highest silver-leaching efficiency across both PCB categories, reaching 71.5% for traditional-architecture phones and 60.8% for new-generation phones. For traditional-architecture PCBs, oxaline achieved a slightly higher final efficiency than ethaline, with values of 54.9% and 53.8%, respectively. The opposite order was observed for new-generation PCBs, with ethaline reaching 51.9% and oxaline 45.4%.

For all three DESs, the silver-leaching efficiency was higher for traditional-architecture PCB fines than for new-generation PCB fines. The difference between categories was 1.9 percentage points for ethaline, 10.7 percentage points for acetine, and 9.5 percentage points for oxaline.

Based on both its higher final leaching efficiency and its faster dissolution kinetics, acetine was selected for the subsequent silver recovery experiments. Although the leaching efficiency was higher for traditional-architecture PCBs, the acetine leachate from new-generation PCB fines was selected for downstream recovery tests because it had a higher initial silver grade. The new-generation fines contained 428.1 g $t^{-1}$ Ag, compared with 206 g $t^{-1}$ in the traditional-architecture fines, and yielded a slightly higher dissolved-silver concentration under the experimental conditions.

### *2.3. Silver Recovery from the Acetine-Loaded Leachate*

Silver recovery from acetine was evaluated using cementation with metallic iron. This method was initially tested using a reference system containing a silver standard and was subsequently applied to the real acetine leachate obtained from new-generation mobile-phone PCB fines.

#### 2.3.1. Silver Recovery by Cementation with Metallic Iron

Table 7 presents the silver recovery after treatment with metallic iron.

**Table 7.** Silver recovery after Fe cementation in the reference system and the real acetine leachate.

| System | Ag Recovery (%) |
|---|---|
| Reference | 98.8 |
| Real acetine leachate | 84.8 |

Silver recovery by cementation with metallic iron reached 98.8% in the reference system. However, the recovery efficiency decreased to 84.8% when the process was applied to the real acetine leachate.

#### 2.3.2. Iron Dissolution During Cementation

The dissolution of the metallic iron used as the cementing agent was evaluated after treatment of both the reference system and the real PCB leachate. In the reference acetine system, total iron dissolution represented 1.2% of the initial 200 mg of iron added to the experiment. Only 12.8% of the dissolved iron was associated with silver cementation. The remaining 87.2% could not be accounted for by silver recovery and was therefore attributed to additional iron dissolution in the acetine medium.

In the real acetine leachate, iron dissolution accounted for 0.54% of the initial iron mass. The stoichiometric balance indicated that approximately 2.8% of the dissolved iron could be associated with silver cementation, whereas the remaining 97.2% may be attributed to other processes, including the potential cementation of other metals present in the DES leachate originating from the PCBs, as well as additional iron dissolution in the acetine medium. Within the uncertainty of the mass balance, the measured iron dissolution could therefore be accounted for by the combined silver- and other metal-cementation reactions.

## 3. Discussion

### *3.1. Silver Grade and Granulochemical Distribution in Mobile-Phone PCBs*

The recalculated silver grade of the traditional-architecture mobile-phone PCBs was 142.5 g $t^{-1}$, considerably lower than the approximately 7900 g $t^{-1}$ reported for comparable PCBs by [31]. This difference may reflect variations in device manufacturer, production year, technological design, and sampling strategy, as well as differences in the analytical procedures used to determine the metal content. In the present study, the PCBs were comminuted, separated into particle-size fractions, and individually analyzed by fire assay, whereas [31] used thermal liberation followed by direct HCl digestion without prior particle-size classification. Because mobile-phone PCBs are highly heterogeneous materials, differences in sample preparation and in the mass analyzed can substantially affect the reported silver grade.

The new-generation PCB sample reached a recalculated silver grade of 569.3 g $t^{-1}$, approximately four times the 142.5 g $t^{-1}$ obtained for traditional-architecture PCBs. The direction of this difference is consistent with [6], which reported average silver contents of 1600 mg $kg^{-1}$ for feature phones and 1732.9 mg $kg^{-1}$ for smartphones. However, the substantially larger difference observed in the present study indicates that the technological category alone may not explain the measured grades. Variations in the models included in each composite sample, in component density, in manufacturing period, and in the heterogeneous distribution of silver-bearing components may also have contributed to the result. Therefore, the reported grades should be interpreted as representative of the specific groups of devices analyzed rather than as universal values for all feature phones and smartphones.

Silver distribution also differed markedly between the two PCB categories. In traditional-architecture PCBs, 65.9% of the total silver was contained in fractions below

150 μm, including the #100- and #180-mesh fractions and fines. This enrichment in the finer fractions suggests preferential liberation of small silver-bearing components or metallic coatings during comminution. Previous studies have shown that metals and polymer–metal composites can exhibit distinct fragmentation behaviors during PCB size reduction, resulting in particle-size-dependent metal distributions [32,33]. Metal distribution in waste PCBs is influenced by equipment type, component composition, and particle size. Previous work has shown that electronic components and bare PCB substrates contain different metal concentrations across granulometric fractions, although no consistent particle-size trend was identified specifically for silver [34]. Therefore, the silver distributions observed in the present study should be considered representative of the device groups analyzed rather than universal granulometric behavior across all mobile-phone PCBs.

In new-generation PCBs, 88.8% of the silver was concentrated in the #60-mesh fraction, with the fines containing a further 10.8%. This narrow distribution suggests that silver was associated with a limited group of components that fragmented within a similar particle-size range. Multilayer ceramic capacitors, contact materials, solder-bearing fragments, and camera-module components are potential sources of silver-bearing phases in modern mobile phones. Nevertheless, no component-level separation or microchemical analysis was performed; consequently, the association of silver with a specific electronic component remains a hypothesis that requires confirmation using techniques such as SEM–EDS, micro-XRF, or automated mineralogical analysis.

No quantifiable doré beads were obtained from the #20-, #35-, and #180-mesh fractions of the new-generation PCBs. Consequently, a silver grade of 0.0 g $t^{-1}$ was assumed for these fractions in the granulochemical balance calculations. However, this assumption does not necessarily imply the complete absence of silver and may have led to an underestimation of the recalculated feed grade.

The silver grades determined in this study were lower than several values reported in the literature for waste mobile-phone PCBs. This difference may be attributed to a combination of factors, including variations in device generation, manufacturer-specific design, material composition, and feed preparation procedures. In addition, the dismantling stage involved removing several components prior to comminution, which may have reduced the contribution of silver-bearing materials to the analyzed fractions. Furthermore, the heterogeneous distribution of precious metals within PCBs means that silver content can vary considerably between devices and between specific PCB fractions. Consequently, substantial differences between literature values and experimentally determined grades are not unexpected.

Another potential factor contributing to the lower silver grades observed in this work is the loss of silver-containing materials during sample preparation. The removal of metallic shields, connectors, soldered components, and other PCB elements prior to grinding and classification may alter the distribution of precious metals within the processed material. Future studies should investigate the distribution of metals among individual PCB components and preparation fractions to establish more detailed silver mass balances.

### *3.2. Silver Leaching with Choline Chloride-Based DESs*

The dissolution of silver in the investigated deep eutectic solvents is likely associated with the formation of silver-chloride complexes in the chloride-rich environment provided by choline chloride. Previous studies have demonstrated that metal dissolution in choline chloride-based DESs is strongly influenced by chloride complexation, which stabilizes dissolved metal ions and promotes their transfer from the solid phase to the liquid phase [19,35].

In chloride-containing media, metallic silver may undergo oxidation followed by complexation, yielding soluble species such as:

$$Ag^0 \rightarrow Ag^+ + e^-$$

$$Ag^+ + 2Cl^- \rightarrow [AgCl_2]^-$$

Depending on chloride activity, higher-order complexes such as $[AgCl_3]^{2-}$ and $[AgCl_4]^{3-}$ may also be present. The formation of these chlorocomplexes reduces the activity of free silver ions and shifts the dissolution equilibrium toward the leached state, enhancing metal extraction [36].

Since all three solvents evaluated in this study contain the same chloride source, the differences in silver extraction efficiency are more likely related to the physicochemical properties imparted by the hydrogen-bond donor. Acetine exhibited the highest silver extraction efficiency, which may be attributed to its lower viscosity and improved mass-transfer characteristics compared with other choline chloride-based DESs. Enhanced diffusion facilitates the transport of chloride ions toward the reaction interface and the removal of dissolved-silver complexes from the particle surface, thereby improving dissolution kinetics [37,38].

In contrast, ethaline (choline chloride–ethylene glycol) showed lower silver dissolution despite its widespread use in metal-processing applications. This behavior suggests that solvent structure and metal–solvent interactions may influence the stability and transport of dissolved-silver species. For oxaline (choline chloride–oxalic acid), the lower extraction efficiency may additionally be related to the strong chelating capacity of oxalate ions, which can alter metal speciation and potentially promote the formation of less soluble intermediate compounds at the solid–liquid interface, thereby limiting further silver dissolution [39].

Under the mild conditions employed in this study (40 °C, without an external oxidizing agent), silver dissolution is likely governed by the combined effects of oxidation by dissolved oxygen, chlorocomplex stabilization, and diffusion within the heterogeneous PCB matrix. Therefore, the superior performance of acetine appears to result from a favorable balance between chloride-mediated silver complexation and solvent transport properties.

Conventional silver recovery processes frequently employ nitric acid-, cyanide-, or thiosulfate-based leaching systems. These technologies have been extensively studied and can achieve high metal recoveries; however, they may involve highly corrosive reagents, pose toxicity concerns, or require complex reagent management. In contrast, choline chloride-based deep eutectic solvents have attracted increasing attention as alternative leaching media due to their low volatility and the possibility of operating under relatively mild conditions. Nevertheless, the present study was not intended to provide a direct comparison between DESs and conventional leaching technologies. Additional studies involving solvent recycling, reagent consumption, recovery efficiency, product quality, environmental performance, and techno-economic analysis would be required before meaningful comparisons can be established.

Acetine achieved the highest and fastest silver-leaching efficiency across both PCB categories, reaching 71.5% for traditional-architecture PCBs and 60.8% for new-generation PCBs after 24 h. In both cases, most silver dissolution occurred during the first 6 h. The efficiency subsequently remained nearly constant, indicating that an apparent plateau had been reached under the conditions evaluated.

The rapid leaching observed with acetine may be related to its physicochemical properties and acidic character. A viscosity of approximately 5.127 mPa·s at 40 °C has been reported for comparable ChCl–acetic acid mixtures [40], whereas ethaline exhibits a higher reported viscosity of approximately 9.50 mPa·s under similar conditions [36]. Lower viscosity can improve mixing and mass transfer between the PCB particles and the liquid phase. The observed performance of acetine is therefore consistent with more favorable

transport properties. Nevertheless, viscosity was not measured experimentally in this study, and the reported values correspond to those of comparable DES systems in the literature. Therefore, differences in silver dissolution cannot be attributed exclusively to viscosity. Acidity, chloride activity, water content, metal complexation, and silver speciation may also play important roles in determining extraction performance.

The plateau observed with acetine after approximately 6 h could result from depletion of readily accessible silver-bearing phases, surface passivation, solvent saturation, or secondary precipitation. The available data do not distinguish among these possibilities. Characterization of the leaching residues and monitoring of silver speciation in the DES would be required to determine the mechanism responsible for the stabilization.

Ethaline exhibited slower kinetics and reached final leaching efficiencies of 53.8% for traditional-architecture PCBs and 51.9% for new-generation PCBs. Neither curve reached a clear plateau within 24 h. Its slower performance is consistent with its higher reported viscosity relative to acetine [41], which may limit mass transfer. The results were lower than the 94.82% silver extraction reported by [42] using a ternary ChCl–ethylene glycol–citric acid DES at 120 °C. The difference is reasonable given the considerably higher temperature, longer or different treatment conditions, and presence of an additional acidic component in the ternary system. The comparison indicates that DES composition and operating temperature strongly influence silver dissolution and that the present experiments were conducted under comparatively mild conditions.

Oxaline achieved 54.9% leaching efficiency for traditional-architecture PCBs and 45.4% for new-generation PCBs after 24 h. The continuously increasing curves suggest that longer contact times could produce additional dissolution. These results are broadly comparable to those of [43], who obtained silver recoveries close to 40% from PCBs using oxaline in the presence of $H_2O_2$. Despite the absence of an externally added oxidant in the present study, oxaline achieved similar or moderately higher efficiencies. Differences in particle size, PCB composition, DES preparation, and experimental conditions prevent a direct quantitative comparison. In addition to the effects of viscosity and mass-transfer limitations, the lower silver extraction observed in oxaline may be associated with the chemistry of oxalate-containing systems. Oxalate ions can interact strongly with dissolved metal species and may promote the formation of sparingly soluble compounds. In particular, the formation of silver oxalate has been reported under suitable conditions and could potentially reduce the concentration of dissolved silver available in the leachate. Although no solid-phase characterization or silver speciation analyses were performed in the present study, this possibility warrants further investigation in future work.

Information on acetine as a leaching medium for electronic waste remains limited. Ref. [25] reported high extraction efficiencies for Cu, Ni, and Au from PCBs using ChCl–acetic acid with iodine as an oxidizing agent under more intensive conditions of 65 °C and 96 h. Although silver was not evaluated in that study, the results demonstrate that acetine can support the dissolution and stabilization of PCB-derived metals. The present results extend its potential application by demonstrating substantial silver leaching at 40 °C without the deliberate addition of an external oxidant.

Silver in PCBs may occur not only as metallic Ag but also in solders, coatings, alloys, or pre-oxidized compounds. Dissolved oxygen, residual oxidizing species in the PCB matrix, or galvanic interactions with other metals could also contribute to the oxidation of silver. Consequently, the present results demonstrate operational silver transfer to the DES but do not establish the mechanism of oxidation or complexation. Electrochemical measurements and solid-phase characterization would be necessary to identify the species involved.

Traditional-architecture PCB fines produced higher silver-leaching efficiencies than new-generation PCB fines for all three DESs, despite having a lower initial silver grade.

The difference was particularly evident for acetine and oxaline. Because the operating conditions and particle-size range were identical, this behavior is more likely attributable to differences in composition, silver-bearing phases, or liberation than to the experimental conditions. Modern PCBs contain highly integrated and multilayered components that may retain metals within ceramic, polymeric, or composite structures even after fine grinding. Reference [30] similarly reported the persistence of incompletely liberated composite particles in fine PCB fractions. Thus, the higher silver grade of the new-generation fines did not necessarily translate into greater percentage dissolution.

Filtration through a 0.22 µm PTFE membrane minimized the possible contribution of suspended PCB particles to the AAS measurements. Nevertheless, the use of aqueous calibration standards without matrix matching or a DES-specific spike-recovery test represents an analytical limitation. Residual matrix effects and possible changes in silver speciation during aqueous dilution cannot therefore be completely excluded, and the reported values should be interpreted as operationally determined dissolved-silver concentrations under the applied sample-preparation and AAS conditions.

Overall, acetine provided the best combination of rapid kinetics and final leaching efficiency. Its selection for the downstream recovery experiments was therefore supported by both kinetic and metallurgical criteria. Nevertheless, the maximum efficiency remained below 72%, indicating that further optimization is necessary. Potential variables include temperature, contact time, solid loading, DES water content, particle size, oxidant addition, and selective removal of copper before silver leaching.

It should also be noted that water was intentionally added during the preparation of oxaline to obtain a homogeneous and stable liquid phase. Consequently, the water content of oxaline differed from that of acetine and ethaline, introducing an additional variable that may affect viscosity, ionic mobility, metal speciation, and overall leaching behavior. Therefore, direct comparison among the three DES systems should be interpreted with caution.

### *3.3. Silver Recovery from the Acetine Leachate*

#### 3.3.1. Cementation with Metallic Iron

Iron cementation also achieved 98.8% silver recovery in the reference acetine system. This result is consistent with the positive standard cell potential for the reaction between the $Ag^+/Ag$ and $Fe^{2+}/Fe$ ($E°cell = +1.24$ V) [44]. Comparable near-complete silver cementation has been reported using iron powder in conventional aqueous leachates [45].

In the real acetine leachate, silver recovery decreased to 84.8%, while copper removal reached 37.3%. Copper cementation on iron is thermodynamically favorable because the standard reduction potential of the $Cu^{2+}/Cu$ couple is more positive than that of $Fe^{2+}/Fe$. Therefore, copper can compete with silver for the available iron surface, particularly when its concentration is substantially higher than that of silver. Simultaneous copper deposition may reduce the number of accessible reaction sites, modify the morphology of the cement layer, and affect mass transfer toward the iron surface.

Silver has a more positive reduction potential than copper and would be expected to cement preferentially under ideal conditions. However, the large concentration difference between Cu and Ag in the real leachate can promote substantial copper reduction. Similar competition between silver and copper during cementation has been reported in conventional hydrometallurgical systems [46,47]. The results, therefore, demonstrate that thermodynamic favorability alone does not ensure selective silver recovery from a concentrated multimetal leachate.

The recovery experiments conducted in this study were intended as a preliminary assessment of the feasibility of recovering silver from DES leachates rather than as a compre-

hensive evaluation or optimization of recovery technologies. The reference system, prepared from a certified silver standard solution, was used to provide a simplified silver-containing medium that enabled examination of the recovery process under controlled conditions prior to testing a real PCB leachate. Although this approach does not reproduce the complete chemical complexity of the DES leachate, it provides a useful baseline for evaluating silver recovery performance.

#### 3.3.2. Iron Dissolution During Cementation

In the reference acetine system, total iron dissolution represented 1.2% of the initial iron mass. The stoichiometric balance indicated that only 12.8% of the dissolved iron was required for the measured silver recovery, with the remaining 87.2% attributable to additional dissolution in the DES. This result indicates that the acidic acetine medium can consume iron independently of the productive cementation reaction. Similar non-selective iron corrosion has been reported in acidic, carboxylic acid-based DESs [48,49].

In the real leachate, total iron dissolution decreased to 0.54%. Based on the stoichiometric balance, approximately 2.8% of the dissolved iron was associated with silver cementation and 97.2% with copper cementation. Under the assumptions used in the balance, no additional iron dissolution was required to explain the measured value. A possible explanation is the formation of a copper-rich deposit that partially isolated the iron surface from the acidic DES. However, this hypothesis cannot be confirmed without surface characterization. Moreover, the balance depends on the accuracy of the copper concentration and the assumed oxidation state of the dissolved species.

Fe cementation produced numerically identical silver recoveries: 98.8% in the reference system and 84.8% in the real leachate. The similarity of the results indicates that the composition of the loaded DESs exerted a greater influence on recovery efficiency than the selected separation mechanism.

Cementation is expected to produce a metallic silver-bearing material directly and has low energy requirements and operational simplicity [50]. However, it consumes iron, introduces dissolved Fe into the solvent, and simultaneously removes copper, reducing product purity.

These findings demonstrate the technical workability of recovering silver from acetine using metallic iron, while also identifying selectivity as the main limitation of the integrated process. Selective copper removal before DES leaching, control of silver and copper speciation, optimization of reagent dosage, and characterization of the recovered solids are necessary before either route can be reliably assessed for scale-up. The regeneration and reuse of acetine must also be evaluated because the accumulation of Cu, Fe, and other dissolved metals may modify its physicochemical properties and leaching performance over successive cycles.

### *3.4. Limitations, Challenges, and Future Perspectives*

Although the results of this study demonstrate the technical feasibility of silver recovery using acetine, the process's long-term viability will depend on the effective regeneration and reuse of the deep eutectic solvent. The present study focused on establishing the extraction and recovery performance of the selected DESs, and, therefore, solvent recycling was beyond its scope. Future investigations should evaluate DES regeneration methods, solvent stability across successive operating cycles, changes in leaching efficiency due to impurity accumulation, and the overall impact of solvent reuse on process economics and environmental sustainability.

While the present study focused exclusively on silver leaching as a first assessment of the applicability of choline chloride-based DESs to waste mobile-phone PCBs, future

research should examine the behavior of additional valuable metals contained in the feed material. In this context, detailed characterization of both the raw PCB fractions and the leaching residues by XRD and SEM-EDS would provide valuable information regarding phase evolution, metal distribution, selective dissolution mechanisms, and opportunities for the sequential recovery of other metallic constituents.

Although the results demonstrate the feasibility of silver recovery using choline chloride-based DESs, the selectivity of the leaching process toward other metallic constituents was not evaluated in the present work. Waste mobile-phone PCBs contain a complex assemblage of valuable and base metals, including copper, gold, nickel, lead, iron, and tin, whose dissolution behavior may significantly influence process efficiency and downstream metal recovery. Future studies should therefore investigate the simultaneous leaching behavior of these elements, quantify metal selectivity, and evaluate possible competitive interactions occurring in DES media. Such investigations will contribute to a more complete understanding of metal speciation, solvent performance, and selective recovery strategies for complex electronic-waste streams.

Silver dissolution in chloride-rich media generally requires an oxidation step followed by stabilization of the dissolved species as silver chlorocomplexes. The absence of an external oxidizing agent may have limited the extraction efficiencies achieved in this study. The objective of the present work was to evaluate the intrinsic leaching behavior of choline chloride-based DESs under simplified conditions; therefore, oxidant-assisted leaching was not investigated. Future studies should examine the effects of oxidizing agents such as $H_2O_2$, $Fe^{3+}$, or oxygen-enriched systems on the generation of $Ag^+$ species and their subsequent complexation as $[AgCl_2]^-$, $[AgCl_3]^{2-}$, and related chlorocomplexes. Such investigations may provide valuable insights into the reaction mechanism and identify opportunities to enhance silver recovery from PCB materials.

Preliminary tests indicated that silver precipitation using sodium chloride may represent a viable alternative for recovering dissolved silver from DES leachates, with recovery levels exceeding 90% under certain experimental conditions. However, this recovery route was not investigated with the same level of detail as the iron cementation process and was therefore not included in the quantitative comparison presented in this work. Future studies should evaluate the influence of operating variables such as chloride concentration, temperature, reaction time, and impurity content on precipitation efficiency and product purity in order to determine the practical applicability of this approach.

Although the present work focused on silver recovery, waste PCB leachates are complex solutions that may contain a variety of dissolved metallic species originating from the boards' electronic components and conductive structures. Besides silver, metals such as copper, tin, lead, nickel, zinc, iron, and others may potentially be solubilized during the leaching process depending on the operating conditions and the composition of the feed material. The presence of these species may influence cementation performance through competing reduction reactions, galvanic interactions, surface passivation, or co-deposition phenomena. Since the concentrations of these metals were not determined in the present study, their effects were not quantitatively evaluated. Future investigations should include multi-element analysis of leachates and solid products to assess process selectivity and interactions between silver and co-dissolved metals during metal recovery.

A limitation of the present study is the incomplete availability of replicate measurements for certain experimental datasets. Given the inherent heterogeneity of waste printed circuit boards and the relatively small sample masses used in leaching tests, variability in particle composition and metal distribution may affect the reported results. Consequently, caution is warranted when interpreting small differences in extraction efficiencies among the investigated systems. Future work should incorporate a more extensive experimental

design with replicated assays and statistical analysis to provide a more rigorous assessment of process performance and variability.

Future investigations should include direct measurements of key physicochemical properties of the DES systems, such as viscosity and water content, as well as solution speciation studies and characterization of reaction products. Such analyses would provide a more comprehensive understanding of the factors controlling silver dissolution and would help distinguish the relative contributions of chloride complexation, solvent transport properties, water content, and possible precipitation phenomena in different DES formulations.

The recovery experiments were conducted under fixed operating conditions, and this study should therefore should not be interpreted as an optimization study. Parameters such as reagent dosage, contact time, temperature, agitation intensity, and surface condition of the cementing agent were not systematically investigated. Future work should evaluate the influence of these variables on recovery efficiency, reaction kinetics, product purity, and process selectivity. Such studies would provide a more rigorous basis for the development and optimization of silver recovery strategies from DES leachates.

Several aspects relevant to process sustainability and industrial implementation were beyond the scope of the present investigation. In particular, the purity and composition of the recovered silver product were not characterized, solvent regeneration and reuse were not evaluated, and reagent consumption was not assessed on a mass-of-silver-recovered basis. Furthermore, the leaching experiments were conducted under laboratory-scale conditions using a relatively low solid-to-liquid ratio. Consequently, the results should be interpreted as a preliminary assessment of technical feasibility rather than a complete evaluation of process sustainability or commercial viability.

## 4. Materials and Methods

### *4.1. Collection, Classification, and Dismantling of Mobile Phones*

Approximately 500 post-consumer mobile phones were collected through an electronic-waste recycling campaign conducted in collaboration with MetalCycle, Quito, Ecuador. The devices were manually classified into two categories based on their technological architecture: traditional-architecture phones with physical keyboards and new-generation phones with touchscreen interfaces.

Each device was manually dismantled by removing the back cover, battery, screen, screws, casing, and other external components. The printed circuit board (PCB) was subsequently separated from the remaining components. This procedure yielded 146 PCBs from traditional-architecture phones and 177 PCBs from new-generation phones.

The steel covers and shields attached to the PCB surfaces were manually removed before comminution to minimize interference during size reduction and subsequent leaching. The cleaned PCBs from the two phone categories were stored and processed separately throughout the experimental procedure.

### *4.2. Size Reduction, Sampling, and Particle-Size Classification*

The PCBs from each phone category were separately comminuted using an Indumei, Ibarra, Ecuador hammer mill. The equipment was cleaned between batches to minimize cross-contamination.

A representative sample of approximately 300 g was obtained from each comminuted batch by successive quartering. Each sample was sieved for 15 min using an ATM Arrow vibratory sieve shaker equipped with #20, #35, #60, #80, #100, and #180 meshes, corresponding to openings of 1700, 850, 425, 250, 180, 150, and 85 µm, respectively. A bottom-pan fraction containing particles smaller than 85 µm was also collected. Sieving was performed twice to obtain sufficient material for subsequent characterization.

The mass retained in each particle-size fraction was recorded. The recalculated silver grade of each PCB category was determined as the mass-weighted average of the silver grades measured in the individual particle-size fractions. The silver distribution in each fraction was calculated as the percentage of the total silver mass contained in that fraction relative to the total silver mass in all analyzed fractions.

### *4.3. Granulochemical Characterization by Fire Assay*

#### 4.3.1. Sulfuric Acid Pretreatment

The #20-, #35-, and #60-mesh fractions were subjected to sulfuric acid pretreatment before fire assay as a sample-preparation step intended to partially remove acid-soluble base-metal components that could interfere with lead-button formation and phase separation during fusion. For each fraction, 30 g of PCB material was brought into contact with 270 mL of 1.5 M $H_2SO_4$, corresponding to a solid loading of 10 wt.%. The suspensions were agitated at 300 rpm for 96 h at room temperature.

After pretreatment, the solids were separated by vacuum filtration, washed with distilled water to remove residual acid, dried, and subsequently analyzed by fire assay.

#### 4.3.2. Fire Assay and Cupellation

A 20 g sample from each particle-size fraction was homogenized with a flux charge consisting of 80 g of a 1:1 mass mixture of sodium carbonate and litharge, 30 g of borax decahydrate, 25 g of silica, 15 g of calcium carbonate, 3 g of flour, and 5 g of potassium nitrate.

The sample–flux mixture was transferred to a crucible and melted in an Optic Ivymen System, Comecta S.A., Abrera, Barcelona, Spain, muffle furnace at 1050 °C for 2 h. The molten material was poured into a mold and allowed to cool to room temperature. When the resulting melt did not exhibit adequate fluidity or phase separation, 10 g of additional borax was added, and the sample was remelted at 1050 °C for another 2 h.

After cooling, the lead button was mechanically separated from the slag and transferred to a preheated cupel. The cupels were initially heated at 1050 °C for 15 min, after which the lead buttons were cupelled at the same temperature for approximately 45 min. The resulting doré beads were collected for chemical analysis.

#### 4.3.3. Doré Digestion and Silver Quantification

Each doré bead was weighed using a BOECO, Hamburg, Germany BAS 31 analytical balance and transferred to a glass digestion tube. Subsequently, 1 mL of distilled water and 1 mL of 70% analytical-grade $HNO_3$ (Fisher Chemical, Fair Lawn, NJ, USA) were added. The samples were heated in a water bath to promote dissolution.

When a doré bead was not completely digested with nitric acid, 3 mL of 37% analytical-grade HCl (Fisher Chemical, Fair Lawn, NJ, USA) was added to form aqua regia, corresponding to an $HCl_3$ volume ratio of 3:1. Heating in the water bath was continued until digestion was complete.

The resulting solutions were transferred to 250 mL volumetric flasks and diluted to volume with distilled water. Silver concentrations were determined by atomic absorption spectrometry using a PerkinElmer, Shelton, CT, USA, AAnalyst 200 instrument. The silver grade of each particle-size fraction was calculated from the measured silver concentration, digestion volume, dilution factors, and initial sample mass.

When no quantifiable doré bead was obtained, a silver grade of 0.0 g $t^{-1}$ was assigned to the corresponding fraction to complete the granulochemical balance.

### *4.4. Preparation and Density Determination of the DESs*

Three deep eutectic solvent systems were prepared using choline chloride (ChCl; ≥98%, Sigma-Aldrich) as the hydrogen-bond acceptor. Acetic acid (AC; ≥98%, Sigma-Aldrich, Steinheim, Germany), oxalic acid (OX; ≥98%, Sigma-Aldrich), and ethylene glycol (EG; analytical grade, Mallinckrodt) were used as hydrogen-bond donors.

Before DES preparation, choline chloride was dried at 80 °C for 1 h in a Carbolite Gero drying oven to reduce residual moisture. The compositions and molar ratios of the prepared systems are presented in Table 8.

**Table 8.** Composition of the prepared choline chloride-based deep eutectic solvents.

| DES | Components | ChCl:HBD Molar Ratio | Composition Used for 10 g of DES |
|---|---|---|---|
| Acetine | ChCl:acetic acid | 1:2 | 5.38 g ChCl + 4.62 g acetic acid |
| Oxaline | ChCl:oxalic acid | 1:1 | 4.63 g ChCl + 2.98 g oxalic acid + 2.39 g distilled water |
| Ethaline | ChCl:ethylene glycol | 1:2 | 5.29 g ChCl + 4.71 g ethylene glycol |

The components of each system were mixed in a glass beaker and heated at 80 °C under continuous magnetic stirring until a transparent and macroscopically homogeneous liquid was obtained, following the procedure described in [51]. The prepared solvents were stored at room temperature until use.

The density of each DES was measured at 25 °C using a 25 mL pycnometer. The clean and dry pycnometer was weighed empty and then filled with the corresponding DES. After the cap was inserted, the excess liquid was removed, and the filled pycnometer was weighed again. The density was calculated by dividing the mass difference between the filled and empty pycnometer by the pycnometer's volume.

Since the physicochemical properties of choline chloride-based DESs are sensitive to composition, particular care was taken during acetine preparation to minimize the loss of acetic acid through evaporation. The DES was prepared in a covered vessel at moderate temperatures (<80 °C) to preserve the system's intended composition.

### *4.5. Silver-Leaching Experiments*

The fines (<85 µm) from both PCB categories were selected for the comparative leaching experiments. Their selection was based on their appreciable silver grades, comparatively low apparent copper interference during the fire assay, small particle size, and suitability for comparing both phone categories under identical experimental conditions.

Six leaching experiments were conducted, corresponding to the three DES formulations and the two PCB categories. Each test was performed using 0.2 g of PCB fines and 10 g of DES, corresponding to a DES solid loading of 20 g $kg^{-1}$. The experiments were carried out in 50 mL ground-glass flasks at 40 °C and 400 rpm for 24 h. No external oxidizing agent was added.

To monitor silver dissolution, 0.2 mL aliquots were withdrawn after 0.5, 1, 2, 4, 6, and 24 h. Before each sampling, agitation was stopped for 5 min to promote preliminary settling of the suspended solids. The aliquots were filtered through a 0.22 µm PTFE membrane filter to remove residual PCB particles, and the withdrawn volume was immediately replaced with 0.2 mL of freshly prepared, silver-free DES of the corresponding composition to maintain a constant nominal liquid volume. Each filtered aliquot was transferred to a 10 mL volumetric flask, acidified with 205 µL of 70% analytical-grade $HNO_3$, and diluted to volume with distilled water, resulting in a nominal dilution factor of 50.

Silver concentrations were determined by atomic absorption spectrometry using a PerkinElmer, Shelton, CT, USA, AAnalyst 200 instrument. Calibration standards were prepared in an aqueous matrix and were not matrix-matched to the diluted DES samples.

No spike-recovery tests or DES-matched certified reference materials were used. Although the 50-fold dilution substantially reduced the DES content introduced into the instrument, residual matrix effects cannot be excluded. Moreover, no independent experiment was conducted to confirm that acidification completely prevented changes in silver speciation or AgCl formation during aqueous dilution.

Because each aliquot was replaced with fresh silver-free DES, the cumulative mass of dissolved silver at each sampling time was calculated as the sum of the silver remaining in the reactor and the silver removed in all preceding aliquots. The initial liquid volume was calculated from the mass of DES added and its experimentally determined density. Silver-leaching efficiency was then calculated as the ratio of the cumulative mass of dissolved silver to the initial mass of silver in the PCB sample. The latter was determined from the mass of PCB fines used and the silver grade of the corresponding particle-size fraction.

The DES exhibiting the highest silver-leaching efficiency and the most favorable dissolution profile was selected for subsequent silver-recovery experiments.

### *4.6. Silver Recovery from Loaded DES*

#### 4.6.1. Preparation of the Reference and Real Systems

Cementation with metallic iron was evaluated using two types of loaded DES. The reference system was prepared with a 1 mg $mL^{-1}$ silver standard solution (Inorganic Ventures AAAG1-1, Christiansburg, VA, USA) to 5 g of DES. This system was used to evaluate silver recovery in the absence of competing metals.

The real system consisted of acetine obtained after leaching the new-generation mobile-phone PCB fines. This leachate was selected based on acetine's performance and the higher initial silver grade of the new-generation fines.

#### 4.6.2. Cementation with Metallic Iron

The theoretical iron requirement was calculated based on the silver-cementation reaction described in the Introduction. An excess of iron was used in the experiments.

For each test, 200 mg of metallic iron wool (No. 5, MARTE Industrias, Quito, Ecuador) was added to 5 g of loaded DES previously heated to approximately 50 °C in a 50 mL Erlenmeyer flask. The mixture was manually agitated for 15 min.

After treatment, a 0.2 mL aliquot of the liquid phase was transferred to a 10 mL volumetric flask, acidified with 205 µL of 70% analytical-grade $HNO_3$, and diluted to volume with distilled water. Residual Ag and Cu concentrations, as well as dissolved Fe, were determined by atomic absorption spectrometry.

Silver recovery was calculated from the difference between the initial and residual silver concentrations relative to the initial silver concentration in the loaded DES.

Total iron dissolution was calculated relative to the initial 200 mg of iron added. The fractions of dissolved iron associated with silver and copper cementation were estimated from the stoichiometry of the respective cementation reactions presented in the Introduction. The difference between the experimentally measured dissolved iron and the amount theoretically required by the cementation reactions was attributed to additional iron dissolution in the DESs.

## 5. Conclusions

Granulochemical characterization demonstrated a strong dependence of silver grade and particle-size distribution on mobile-phone architecture. New-generation PCBs exhibited a recalculated silver grade of 569.3 g $t^{-1}$, approximately four times higher than the 142.5 g $t^{-1}$ obtained for traditional-architecture PCBs. This difference underscores the importance of category-based sorting in generating more homogeneous, higher-grade feed

streams prior to metallurgical treatment. Silver was distributed mainly among the finer fractions of traditional-architecture PCBs, with 65.8% occurring below 150 µm, whereas 88.8% of the silver in new-generation PCBs was concentrated in the #60 mesh fraction. These distributions may be associated with keypad contacts and solder joints in traditional phones and with multilayer ceramic capacitors or other surface-mounted components in new-generation devices. However, these interpretations remain hypotheses that require confirmation using techniques such as SEM–EDS. Nevertheless, the results support particle-size-targeted processing instead of whole-board treatment.

Among the three DESs evaluated, acetine exhibited the fastest dissolution profile and the highest silver-leaching efficiencies, reaching 71.5% for traditional-architecture PCBs and 60.8% for new-generation PCBs after 24 h. Its superior performance may be related to more favorable mass-transfer conditions than those of ethaline and oxaline. The recovery achieved without adding an external oxidizing agent demonstrates acetine's capacity to directly leach silver from post-consumer mobile-phone PCBs. Traditional-architecture PCBs consistently exhibited higher leaching efficiencies than new-generation PCBs in all three DESs. This behavior may be associated with differences in silver-bearing components and incomplete liberation of silver from composite particles.

The iron mass balance showed that only 12.8% of the dissolved iron in the reference system was theoretically attributable to productive silver cementation, indicating that most of the measured iron dissolution resulted from additional interactions between metallic iron and the DESs. In the real leachate, the stoichiometric analysis attributed approximately 2.8% of the dissolved iron to silver cementation and 97.2% to copper cementation, with little calculated excess iron dissolution. Because the initial copper concentration was estimated and the recovered solids were not characterized, these contributions should be regarded as theoretical estimates. Future SEM–EDS and mineralogical analyses of the cemented products are required to verify the proposed co-deposition mechanism and determine whether the deposited metallic layer restricts further contact between the DES and the iron surface.

The recovery tests demonstrated the feasibility of recovering dissolved silver via iron cementation; however, the results should be interpreted as a proof of concept rather than a comparative assessment of competing recovery methods.

From a product perspective, cementation is advantageous because it recovers silver in metallic form. Overall, this study demonstrates the feasibility of a DES-mediated hydrometallurgical route based on acetine leaching followed by iron cementation for recovering silver from post-consumer mobile-phone PCBs.

**Author Contributions:** Conceptualization, C.F.A.-T., K.M. and F.S.; methodology, C.F.A.-T., P.H. and K.M.; validation, E.M., C.F.A.-T. and K.M.; formal analysis, E.M., C.F.A.-T., K.M. and F.S.; investigation, E.M. and F.S.; resources C.F.A.-T., K.M., F.S., P.H. and E.d.l.T.; writing—original draft preparation, E.M., K.M. and F.S.; writing—review and editing, K.M., F.S. and P.H.; visualization, F.S. and K.M.; supervision, C.F.A.-T. and K.M.; project administration, E.d.l.T.; funding acquisition, E.d.l.T. and C.F.A.-T. All authors have read and agreed to the published version of the manuscript.

**Funding:** The research presented in this study was made possible by financing from the Department of Extractive Metallurgy (DEMEX) of the Escuela Politécnica Nacional thanks to the research project PIS-24-05 "Recuperación Sostenible de Metales Estratégicos: Litio, Cobalto, Neodimio, Cobre y Oro a partir de RAEE con Solventes Ecológicos".

**Data Availability Statement:** The original contributions presented in this study are included in the article. Further inquiries can be directed to the corresponding author.

**Acknowledgments:** The authors would like to express their sincere gratitude to the Escuela Politécnica Nacional for their support in the development of this research. Special thanks are extended to the

Laboratorio de Análisis Químico y Mineralógico del Departamento de Metalurgia Extractiva for providing the technical facilities and assistance necessary for conducting the experimental work.

**Conflicts of Interest:** The authors declare no conflicts of interest. The funders had no role in the design of the study; in the collection, analyses, or interpretation of data; in the writing of the manuscript; or in the decision to publish the results.

## References

1. The Silver Institute. Silver Industrial Demand Rose 11 Percent to Post a New Record in 2023. Available online: https://silverinstitute.org/silver-industrial-demand-rose-11-percent-to-post-a-new-record-in-2023/ (accessed on 22 September 2026).
2. Covaci, C.; Gontean, A. 'Singing' multilayer ceramic capacitors and mitigation methods—A review. *Sensors* **2022**, *22*, 3869. [CrossRef] [PubMed]
3. Chang, Y.C.; Zhang, Y.; Wang, L.; Wang, S.; Wang, H.; Huang, C.Y.; Chen, R.; Chan, C.; Hallam, B. Silver-lean metallization and hybrid contacts via plating on screen-printed metal for silicon solar cells manufacturing. *Prog. Photovolt. Res. Appl.* **2025**, *33*, 158–169. [CrossRef]
4. Baldé, C.P.; Kuehr, R.; Yamamoto, T.; McDonald, R.; Althaf, S.; Bel, G.; Deubzer, O.; Fernandez-Cubillo, E.; Forti, V.; Gray, V.; et al. *The Global E-Waste Monitor 2024*; International Telecommunication Union and United Nations Institute for Training and Research: Geneva, Switzerland/Bonn, Germany, 2024.
5. World Health Organization. Electronic Waste (e-Waste). Available online: https://www.who.int/news-room/fact-sheets/detail/electronic-waste-(e-waste) (accessed on 22 September 2026).
6. Singh, N.; Duan, H.; Yin, F.; Song, Q.; Li, J. Characterizing the materials composition and recovery potential from waste mobile phones: A comparative evaluation of cellular and smart phones. *ACS Sustain. Chem. Eng.* **2018**, *6*, 13016–13024. [CrossRef]
7. Mishra, G.; Jha, R.; Rao, M.D.; Meshram, A.; Singh, K.K. Recovery of silver from waste printed circuit boards (WPCBs) through hydrometallurgical route: A review. *Environ. Chall.* **2021**, *4*, 100073. [CrossRef]
8. Loyo, C.; Arroyo, C.; Aldás, M.; Montero, R. Extracción y caracterización de la fracción no metálica de las tarjetas de circuitos impresos de computadoras desechadas. *Rev. Politéc.* **2015**, *36*, 67.
9. Kootenay Silver Inc. *Mineral Resource Estimate Update for the La Cigarra Ag-Pb-Zn Project, Chihuahua State, Mexico*; Technical Report; Kootenay Silver Inc.: Vancouver, BC, Canada, 2024.
10. Cucchiella, F.; D'Adamo, I.; Koh, S.C.L.; Rosa, P. Recycling of WEEEs: An economic assessment of present and future e-waste streams. *Renew. Sustain. Energy Rev.* **2015**, *51*, 263–272. [CrossRef]
11. Kumari, S.; Panda, R.; Prasad, R.; Alorro, R.D.; Jha, M.K. Sustainable process to recover metals from waste PCBs using physical pre-treatment and hydrometallurgical techniques. *Sustainability* **2024**, *16*, 418. [CrossRef]
12. Hagelüken, C.; Corti, C.W. Recycling of gold from electronics: Cost-effective use through 'design for recycling'. *Gold Bull.* **2010**, *43*, 209–220. [CrossRef]
13. Petter, P.M.H.; Veit, H.M.; Bernardes, A.M. Evaluation of gold and silver leaching from printed circuit board of cellphones. *Waste Manag.* **2014**, *34*, 475–482. [CrossRef] [PubMed]
14. Kuyucak, N.; Akcil, A. Cyanide and removal options from effluents in gold mining and metallurgical processes. *Miner. Eng.* **2013**, *50–51*, 13–29. [CrossRef]
15. Musariri, B.; Akdogan, G.; Dorfling, C.; Bradshaw, S. Evaluating organic acids as alternative leaching reagents for metal recovery from lithium ion batteries. *Miner. Eng.* **2019**, *137*, 108–117. [CrossRef]
16. Nkechi, N.; Theresa, O.; Mark, A.A.; Okoye-Anigbogu, S.M.; Chukwueke, N. Selective recovery of silver from cell phone and television printed circuit boards via organic acids. *J. Mater. Sci. Res. Rev.* **2025**, *8*, 782–794. [CrossRef]
17. Panda, P.; Mishra, S. Deep eutectic solvents: Physico-chemical properties and their use for recovery of metal values from waste products. *J. Mol. Liq.* **2023**, *390*, 123070. [CrossRef]
18. Marcus, Y. *Deep Eutectic Solvents*; Springer International Publishing: Cham, Switzerland, 2019. [CrossRef]
19. Abbott, A.P.; Capper, G.; Davies, D.L.; Rasheed, R.K.; Tambyrajah, V. Novel solvent properties of choline chloride/urea mixtures. *Chem. Commun.* **2003**, 70–71. [CrossRef] [PubMed]
20. Jenkin, G.R.T.; Al-Bassam, A.Z.M.; Harris, R.C.; Abbott, A.P.; Smith, D.J.; Holwell, D.A.; Chapman, R.J.; Stanley, C.J. The application of deep eutectic solvent ionic liquids for environmentally-friendly dissolution and recovery of precious metals. *Miner. Eng.* **2016**, *87*, 18–24. [CrossRef]
21. Moganti, L.K.; Dutta, D. Deep eutectic solvents in E-waste recycling: Preparation, properties, and hydrometallurgical metal recovery. *RSC Adv.* **2026**, *16*, 5228–5251. [CrossRef] [PubMed]
22. Lemoine, C.; Petit, Y.; Karaman, T.; Jahrsengene, G.; Martinez, A.M.; Benayad, A.; Billy, E. Circular recycling concept for silver recovery from photovoltaic cells in Ethaline deep eutectic solvent. *RSC Adv.* **2024**, *14*, 29174–29183. [CrossRef] [PubMed]

23. Khuduwe, M.J.; Shemi, A.; Ndlovu, S. Extraction of gold from tailings using Ethaline deep eutectic solvent. *Minerals* **2024**, *14*, 1239. [CrossRef]
24. Guamán-Gualancañay, J.M.; Aragón-Tobar, C.F.; Moreno, K.; Palacios, J.L.; Endara, D. Recovery of lithium and cobalt from spent lithium-ion batteries using a deep eutectic solvent based on choline chloride and oxalic acid (Oxaline). *Molecules* **2025**, *30*, 4690. [CrossRef] [PubMed]
25. Saffaj, S.; Mantovani, D.; Kolliopoulos, G. Sustainable leaching of Cu, Ni, and Au from waste printed circuit boards using choline chloride-based deep eutectic solvents. *Metals* **2025**, *15*, 82. [CrossRef]
26. Park, Y.J.; Fray, D.J. Recovery of high purity precious metals from printed circuit boards. *J. Hazard. Mater.* **2009**, *164*, 1152–1158. [CrossRef] [PubMed]
27. Zhang, C.; Jiang, J.; Ma, E.; Zhang, L.; Bai, J.; Wang, J.; Bu, Y.; Fan, G.; Wang, R. Recovery of silver from crystal silicon solar panels in self-synthesized choline chloride–urea solvent system. *Waste Manag.* **2022**, *150*, 280–289. [CrossRef] [PubMed]
28. Djoudi, W.; Aissani-Benissad, F.; Bourouina-Bacha, S. Optimization of copper cementation process by iron using central composite design experiments. *Chem. Eng. J.* **2007**, *133*, 1–6. [CrossRef]
29. Gerold, E.; Lerchbammer, R.; Antrekowitsch, H. Evaluation of the influence exerted by increased silicon contents on the leaching behavior of NMC-based black mass. *Metals* **2023**, *13*, 785. [CrossRef]
30. Ogunniyi, I.O.; Vermaak, M.K.G.; Groot, D.R. Chemical composition and liberation characterization of printed circuit board comminution fines for beneficiation investigations. *Waste Manag.* **2009**, *29*, 2140–2146. [CrossRef] [PubMed]
31. Vats, M.C.; Singh, S.K. Assessment of gold and silver in assorted mobile phone printed circuit boards (PCBs). *Waste Manag.* **2015**, *45*, 280–288. [CrossRef] [PubMed]
32. Grimmenstein, J.E.; Trebeck, E.; Krampitz, T.; Lieberwirth, H. Recycling through comminution: Characterization, separation and recycling barriers of metal-coated polymers and metallized polymer foams. *Recycling* **2024**, *9*, 120. [CrossRef]
33. Oliveira, P.C.; Cabral, M.; Nogueira, C.A.; Margarido, F. Printed circuit boards recycling: Characterization of granulometric fractions from shredding process. *Mater. Sci. Forum* **2010**, *636–637*, 1434–1439. [CrossRef]
34. Anić-Vučinić, A.; Bedeković, G.; Šarc, R.; Premur, V. Determining metal content in waste printed circuit boards and their electronic components. *J. Sustain. Dev. Energy Water Environ. Syst.* **2020**, *8*, 590–602. [CrossRef]
35. Abbott, A.P.; Barron, J.C.; Ryder, K.S.; Wilson, D. Eutectic-based ionic liquids with metal-containing anions and cations. *Chem. Eur. J.* **2007**, *13*, 6495–6501. [CrossRef] [PubMed]
36. Aylmore, M.G.; Muir, D.M. Thiosulfate leaching of gold—A review. *Miner. Eng.* **2001**, *14*, 135–174. [CrossRef]
37. Smith, E.L.; Abbott, A.P.; Ryder, K.S. Deep eutectic solvents (DESs) and their applications. *Chem. Rev.* **2014**, *114*, 11060–11082. [CrossRef] [PubMed]
38. Abbott, A.P.; Frisch, G.; Hartley, J.; Ryder, K.S. Processing of metals and metal oxides using ionic liquids. *Green Chem.* **2011**, *13*, 471–481. [CrossRef]
39. Paiva, A.; Craveiro, R.; Aroso, I.; Martins, M.; Reis, R.L.; Duarte, A.R.C. Natural deep eutectic solvents—Solvents for the 21st century. *ACS Sustain. Chem. Eng.* **2014**, *2*, 1063–1071. [CrossRef]
40. Sheikh, A.; Khan, A.Y.; Ahmed, S. Physicochemical properties of choline chloride/acetic acid as a deep eutectic solvent and its binary solutions with DMSO at 298.15 to 353.15 K. *ACS Omega* **2024**, *9*, 3730–3745. [CrossRef] [PubMed]
41. Harifi-Mood, A.R.; Buchner, R. Density, viscosity, and conductivity of choline chloride + ethylene glycol as a deep eutectic solvent and its binary mixtures with dimethyl sulfoxide. *J. Mol. Liq.* **2017**, *225*, 689–695. [CrossRef]
42. Fatimah, S.S.; Simanungkalit, Y.A.; Risdianto, M.R.C.; Alhaqqa, J.Y.; Sumarna, O.; Mora, A. Silver leaching from wasted printed circuit boards using choline chloride-based ternary deep eutectic solvents. *Physicochem. Probl. Miner. Process.* **2026**, *62*, 219012. [CrossRef]
43. Emmons-Burzyńska, M.; Jędrzejczak, E.; Piasecki, A.; Ławniczak, Ł.; Regel-Rosocka, M.; Wysokowski, M. Leaching of metals from electronic waste using carboxylic acid-based deep eutectic solvents: Preliminary laboratory studies and molecular modelling. *Hydrometallurgy* **2025**, *234*, 106465. [CrossRef]
44. Bard, A.J.; Faulkner, L.R. *Electrochemical Methods: Fundamentals and Applications*, 2nd ed.; John Wiley & Sons: New York, NY, USA, 2001.
45. Ehsani, A.; Yazıcı, E.Y.; Deveci, H. Precipitation of silver from copper sulphate solutions. In Proceedings of the International Black Sea Mining & Tunnelling Symposium, Trabzon, Turkey, 2–4 November 2016.
46. Kim, B.J.; Cho, K.H.; Choi, N.C.; Park, C.Y. The recovery of silver from thiourea leaching solution by cementation technique. *Econ. Environ. Geol.* **2013**, *46*, 29–37. [CrossRef]
47. Zante, G.; Boltoeva, M. Review on hydrometallurgical recovery of metals with deep eutectic solvents. *Sustain. Chem.* **2020**, *1*, 238–255. [CrossRef]
48. García-Díaz, I.; Alguacil, F.J.; López, F.A. Tin and silver recovery from wave soldering dross. *Waste Manag. Res.* **2018**, *36*, 1201–1209. [CrossRef] [PubMed]

49. Ahmed, E.I.; Ryder, K.S.; Abbott, A.P. Corrosion of iron, nickel and aluminium in deep eutectic solvents. *Electrochim. Acta* **2021**, *397*, 139284. [CrossRef]
50. Hussain, J.; Sim, M.; Rosaiah, P.; Hussain, I. A review of sustainable cementation strategies for precious metal recovery: Efficiency, environmental impact and future prospects. *J. Hazard. Mater. Adv.* **2026**, *22*, 101120. [CrossRef]
51. Aragón-Tobar, C.F.; Endara, D.; de la Torre, E. Dissolution of metals (Cu, Fe, Pb, and Zn) from different metal-bearing species (sulfides, oxides, and sulfates) using three deep eutectic solvents based on choline chloride. *Molecules* **2024**, *29*, 290. [CrossRef] [PubMed]

**Disclaimer/Publisher's Note:** The statements, opinions and data contained in all publications are solely those of the individual author(s) and contributor(s) and not of MDPI and/or the editor(s). MDPI and/or the editor(s) disclaim responsibility for any injury to people or property resulting from any ideas, methods, instructions or products referred to in the content.